Anticrossing semiconducting band gap in nominally semimetallic InAs/GaSb superlattices

Rita Magri, L. W. Wang, and Alex Zunger
National Renewable Energy Laboratory, Golden, Colorado 80401

I. Vurgaftman and J. R. Meyer
Naval Research Laboratory, Washington, D.C. 20375

(Received 17 September 1999)

While $(InAs)_n/(GaSb)_n$ (001) superlattices are semiconducting for $n<n_c\approx 28$ ML, for $n>n_c$ the InAs electron level e_{InAs} is below the GaSb hole level h_{GaSb}, so the system is converted to a nominal semimetal. At nonzero in-plane wave vectors ($\mathbf{k}_\parallel\neq 0$), however, the wave functions e_{InAs} and h_{GaSb} have the same symmetry, so they anticross. This opens up a ''hybridization gap'' at some $\mathbf{k}_\parallel=\mathbf{k}_\parallel^*$. Using a pseudopotential plane-wave approach as well as a (pseudopotential fit) eight-band $\mathbf{k}\cdot\mathbf{p}$ approach, we predict the hybridization gap and its properties such as wave-function localization and out-of-plane dispersion. We find that recent model calculations underestimate this gap severely.

I. INTRODUCTION

On an absolute energy scale, the valence-band maximum (VBM) of GaSb is higher in energy than the conduction-band minimum (CBM) of InAs.[1] Consequently, a GaSb/InAs heterojunction should be metallic, with the InAs-localized electron levels e_{InAs} *below* the GaSb-localized hole level h_{GaSb}. In $(InAs)_n/(GaSb)_n$ superlattice geometry, quantum confinement will push e_{InAs} to *higher* energies and h_{GaSb} to *lower* energies, thus opening up a semiconducting band gap at sufficiently small periods $n<n_c$. Early experiments[2,3] indeed suggested a transition from semiconductor at $n<n_c$ to semimetal at $n>n_c$. However, in 1983, Altarelli[4] pointed out that even for $n>n_c$ there could be a semiconducting gap: since at some in-plane wave vector $\mathbf{k}_\parallel$ the states e_{InAs} and h_{GaSb} have the same symmetry representation, they must *anticross* (rather than cross), thus opening a finite gap. [Here $\mathbf{k}_\parallel=(k_x,k_y)$ indicates the transverse, two-dimensional wave vector parallel to the substrate plane, while k_z denotes the wave vector component parallel to the superlattice growth direction. The Brillouin zone is shown in Fig. 1.] Performing calculations in the $\mathbf{k}\cdot\mathbf{p}$ envelope function approximation (EFA), Altarelli[4] found indeed a semiconducting gap even for $n>n_c$ at some in-plane wave vectors $\mathbf{k}_\parallel^*$. Previous experimental observations of semimetallic behavior[2,3] were interpreted by Altarelli[4] as being due to the abundant defects that fill in the band-gap region. In 1997, Yang *et al.*[5] indeed detected, using capacitance-voltage measurements on $(InAs)_{46}/(GaSb)_{14}$ superlattices, a small band gap ($\approx$4 meV) in the in-plane dispersion. This has prompted theoretical interest in predicting the semiconducting gap of nominally semimetallic superlattices.[6–8] In this paper we use a pseudopotential plane-wave approach to predict the hybridization gap and its properties such as wave function localization and dispersion relations. We also compare our results to those obtained by approximate models such as eight-band $\mathbf{k}\cdot\mathbf{p}$ (finding good agreement, provided that the parameters are drawn from pseudopotential calculations), and to a recent model calculation by de-Leon *et al.*[6] (finding poor agreement). We also find that whereas Altarelli's model predicts but one hybridization gap thus suggesting semiconducting (rather than semimetallic) behavior at $n>n_c$, our multiband model shows that for long period superlattices there are multiple anticrossings. This would lead to a quasisemimetallic behavior, not semiconducting.

II. SYMMETRY-MANDATED BAND COUPLING AND ANTICROSSING IN III-V SUPERLATTICES

Since the semiconducting gap represents anticrossing between two levels, one must understand and predict the effective coupling potential $V_{e\text{-}hh}^{(n)}(\mathbf{k}_\parallel,k_z)$ between the relevant anticrossing states.

There are three outstanding problems of anticrossing and band coupling in semiconductor superlattice physics, that were treated in the past by the ''standard model,'' i.e., EFA.

(i) *The $\Gamma-X$ coupling $V_{\Gamma,X}$ in $(AlAs)_n/(GaAs)_n$ (001) superlattices*, which leads to anticrossing of Γ_{1c}-like and

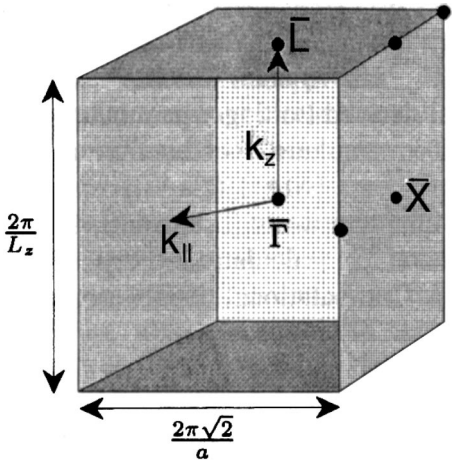

FIG. 1. Brillouin zone for the tetragonal symmetry of the $(InAs)_n/(GaSb)_m$ (001) superlattices. The crystal primitive cell along the z axis is of length $L_z=(n+m)a$ and a is the zinc-blende lattice constant.

X_{1c}-like levels in superlattices, as one applies pressure,[9(a)] electric,[9(b)] or magnetic[9(c)] fields. This nonzero coupling can be described via atomistic theories such as tightbinding[10] or pseudopotentials,[11] but vanishes in the standard model EFA:

$$V_{\Gamma,X}^{EFA}=0. \tag{1}$$

Pseudopotential calculations[11] quantitatively predicted this coupling potential vs the superlattice period n, showing that it vanishes for $n=$ odd, and obtaining the effects of pressure is in good agreement with experiment.

(ii) *The light-hole to heavy-hole coupling $V_{lh,hh}$ in* (001) *superlattices*, which leads at $\mathbf{k}_\parallel=0$ to the observed[12,13] anticrossing of lh_1 with hh_2 excitons. In the D_{2d} point group symmetry of a (001) superlattice having a *common atom* (such as AlAs/GaAs), or in the C_{2v} symmetry of *non-common-atom* (001) superlattices such as InAs/GaSb, the lh_1 and hh_2 states have the same Γ_7 symmetry representation, so they must anticross rather than cross. Atomistic theories such as tightbinding[14] and pseudopotential[15,16] for the D_{2d} superlattices, and pseudopotential[8] theory for the C_{2v} superlattices, indeed produce[8,14–16] anticrossing at $\mathbf{k}_\parallel=0$ [see Fig. 3(b) in Ref. 8]. On the other hand, the standard EFA, being a continuum theory, lacks this anticrossing at $\mathbf{k}_\parallel=0$, since it assumes

$$V_{lh,hh}^{EFA}(\mathbf{k}_\parallel=0)=0 \tag{2a}$$

and

$$V_{lh,hh}^{EFA}(\mathbf{k}_\parallel\neq 0)\neq 0. \tag{2b}$$

The effects of the $V_{lh,hh}(\mathbf{k}_\parallel=0)$ coupling are amplified enormously in C_{2v} non-common-atom superlattices such as GaInAs/InP (001) or InAs/GaSb (001) and reveal themselves through a giant in-plane polarization anisotropy in the optical absorption,[17] which is not present in D_{2d} superlattices. While atomistic models *force* lh-hh mixing at $\mathbf{k}_\parallel=0$ upon us by the very nature of the symmetry properties of the relevant states, such mixing can only be *accommodated* in the standard model of EFA if additional terms are added ''by hand'' to the boundary conditions at the interface[18] or to the EFA Hamiltonian.[17] The theory itself does not provide the magnitude of $V_{lh,hh}(\mathbf{k}_\parallel=0)$, which thus needs to be supplied externally.

(iii) *The electron–heavy-hole coupling $V_{e,hh}$ in non-common-atom superlattices* that leads (a) at $\mathbf{k}_\parallel=0$, to a small anticrossing gap at $n=n_c$[8] as well as to an in-plane polarization anisotropy in the optical absorption[8] and (b) at $\mathbf{k}_\parallel\neq 0$ to the ''hybridization gap'' for $n>n_c$.[5] Again, atomistic theories predict the $\mathbf{k}_\parallel=0$ anticrossing gap and the $\mathbf{k}_\parallel=0$ polarization anisotropy.[8,19] The standard model of EFA, however, results in

$$V_{e,hh}^{EFA}(\mathbf{k}_\parallel=0)=0 \tag{3a}$$

and

$$V_{e,hh}^{EFA}(\mathbf{k}_\parallel\neq 0)\neq 0. \tag{3b}$$

So while EFA-based methods can explain at least qualitatively the in-plane $\mathbf{k}_\parallel\neq 0$ hybridization gap underlying Eq. (3b), they cannot account for the anticrossing behavior at $\mathbf{k}_\parallel=0$ for $n=n_c$ (electron and hole states cross in EFA rather than anticross) nor the $\mathbf{k}_\parallel=0$ polarization anisotropy. Note that Eq. (3a) is a consequence of the fact that $V_{lh,hh}^{EFA}(\mathbf{k}_\parallel=0)=0$. Again, it is possible to add by hand additional terms to EFA to introduce the missing band couplings.[20] However, the value of the coupling constant is undetermined by that theory.

III. CALCULATION OF THE HYBRIDIZATION GAP

We see from the forgoing discussion that the problem of predicting the hybridization gap in non-common-atom superlattices is relatively easy, because already the standard model grants a nonzero coupling in Eq. (3b). This should be contrasted with the more difficult problems of predicting the $\mathbf{k}_\parallel=0$ lh-hh coupling [Eq. (2a)] or the $\Gamma-X$ coupling [Eq. (1)], where, by itself, the standard model provides a null effect. However, the problem of determining the hybridization gap is not entirely trivial, because it is not obvious whether EFA gives the right *magnitude* of the gap. There are two reasons to raise this question: (1) The absence of $V_{e,hh}^{EFA}(\mathbf{k}_\parallel=0)$ can affect the $V_{e,hh}(\mathbf{k}_\parallel\neq 0)$ coupling and thus the hybridization gap at $\mathbf{k}_\parallel\neq 0$; (2) the e-hh coupling comes from the interaction between the InAs-localized electron state and the GaSb-localized heavy-hole state. The magnitude of these couplings sensitively depends on the detailed boundary conditions used at the interface, which are an unsettled issue in the EFA theory.[18,21,22]

While EFA-based models of band coupling involve complex discussions of various boundary condition choices (e.g., see Refs. 6, 18, 21, and references therein), atomistic models are free from such ambiguity, directly provide the magnitude of the coupling constants, and are simple to apply. Recent pseudopotential calculations on $(\mathrm{InAs})_n/(\mathrm{GaSb})_n$ (001) superlattices[8] indeed demonstrated (1) the existence of in-plane polarization anisotropy of the e-hh transitions at $\mathbf{k}_\parallel=0$; (2) the occurence of $e1$-hh1 mixing at $\mathbf{k}_\parallel=0$ around $n=28$; and (3) the anticrossing of the second and third hole states lh1 and hh2 at $\mathbf{k}_\parallel=0$. Because of Eq. (3a) these properties could not be predicted by the standard $\mathbf{k}\cdot\mathbf{p}$ approach. Here we use the same pseudopotential model to study the $\mathbf{k}_\parallel\neq 0$ dispersion in $(\mathrm{InAs})_n/(\mathrm{GaSb})_m$ superlattices strained to the lattice constant of a GaSb substrate, thus determining the anticrossing gap.

In the pseudopotential theory (P theory) used here,[8] the single-particle Schrödinger equation is given by

$$\left[-\frac{\beta}{2}\nabla^2+\sum_{n\alpha} v_\alpha(r-R_{n\alpha})\right]\psi_i(r)=\epsilon_i\psi_i(r), \tag{4}$$

where $R_{n\alpha}$ denotes the position of the nth atom of type α. The atomic positions are determined by minimizing the atomistic strain energy of the superlattice.[8] This results in the InAs and GaSb segments having tetragonal c/a ratios close to one, whereas the two interfaces have a dilated InSb bond ($c/a=1.13$) and a compressed GaAs bond ($c/a=0.85$). The screened pseudopotentials $\{v_\alpha\}$ are determined[8] by fitting to the measured *all-zone* (i.e., not just Γ) bulk band structures of InAs and GaSb (including anisotropic effective masses), and to the local-density approximation (LDA) calculated band offsets and deformation potentials. Spin-orbit interactions are included as a nonlocal part of v_α. The coefficient β

of Eq. (4) is a scale factor selected to improve the simultaneous fit of bulk effective masses and band gaps. This is because the transition matrix element $|\langle\psi_{VBM}|\mathbf{p}|\psi_{CBM}\rangle|^2$, which is denoted $E_p/2$ in $\mathbf{k}\cdot\mathbf{p}$ theory, is too small otherwise. The smallness of E_p is not due to any inaccuracy of the wave functions (which are extremely similar to LDA wave functions). Rather it is due to the fundamental problem of using a local potential to describe the quasiparticle Hamiltonian. The angular-momentum nonlocality of the atomic pseudopotentials will not change this fact because angular momenta nonlocality is used just to compensate the effects of core electrons. Indeed a quasiparticle experiences a self-energy term,[23] which can only be expressed as a general nonlocal potential. To the lowest-order approximation, this type of spatial nonlocality can be expanded in reciprocal space as a kinetic energy term.[24] Thus, we have used a scaling factor β in Eq. (4) to represent this effect. This procedure also increases E_p into the experimental range.

We solve Eq. (4) by expanding ψ_i in a set of plane waves, and solving the eigenstates near the band gap using the folded spectrum method.[25] In parallel, we also performed 8 $\times$8 $\mathbf{k}\cdot\mathbf{p}$ calculations[26,8] in which the Hamiltonian parameters are derived, for purposes of consistency, from the bulk band structures of InAs and GaSb given by $\{v_\alpha\}$. Full details of the performance of this pseudopotential are given in Ref. 8. Our pseudopotential provides a better fit to the properties of InAs and GaSb than the recent empirical pseudopotential method (EPM) of Dente and Tilton.[27] More importantly, our EPM fits continously all momentum values in $v_\alpha(q)$, whereas their potential is fit only at the *bulk* reciprocal lattice vectors, leaving the values at the *superlattice* reciprocal lattice vectors undetermined by the fitting procedure. Indeed, their pseudopotential produces systematically lower band gaps for short-period $(\mathrm{InAs})_n/(\mathrm{GaSb})_n$ (001) superlattices than ours.

IV. RESULTS

A. Pseudopotential band structure, wave functions, and polarization resolved transitions for $(\mathrm{InAs})_{46}(\mathrm{GaSb})_{14}$

The solid colored lines in Fig. 2(a) describe the band structure of $(\mathrm{InAs})_{46}(\mathrm{GaSb})_{14}$. (We have chosen this superlattice because it was measured in Ref. 5.) On the right side, we show the in-plane dispersion along the [1,1] direction ($k_x=k_y$) corresponding to the $k_z=0$ plane, while on the left side we show the in-plane ($k_x=k_y$) dispersion corresponding to $k_z=\pi/L_z$. In the center part we give the dispersion with k_z from $\bar{\Gamma}$ to $\bar{L}$ (see Fig. 1 for the Brillouin zone). Away from $\mathbf{k}_\parallel=0$ the pseudopotential bands split into their spin-orbit components. We color coded the lines according to the localization of the corresponding wave functions. Blue denotes localization in the InAs layer, while red denotes localization in the GaSb layer. We calculated the degree of localization from the spatial variations of the square of the planar-averaged wave functions along the superlattice growth direction (Fig. 3). We concentrate mainly on the two bands indicated in Fig. 2 as ''CBM'' and ''VBM.'' At $\mathbf{k}_\parallel=0$ the CBM is the lower band and has an e_{InAs} character, while the higher VBM band has a h_{GaSb} character. As we move along the in-plane $\mathbf{k}_\parallel$ directions, these bands anticross at some $\mathbf{k}_\parallel^*\neq 0$, forming a hybridization gap, after which the wave functions exchange their character: the lower band becomes h_{GaSb} (red), while the higher becomes e_{InAs} (blue). The evolution of the wave functions of the two bands along the $k_x=k_y$ direction, for $k_z=0$, is shown in Fig. 3. We start at $\mathbf{k}_\parallel=0$, where the lower-energy band indicated as ''CBM'' is localized on the InAs layer, while the higher-energy band, indicated as ''VBM'' is localized on the GaSb layer. As the distance from $\mathbf{k}_\parallel=0$ increases, we see that the localization of the CBM wave function on InAs diminishes, and the wave function acquires more and more weight on the GaSb segment. The opposite is true for the wave function indicated as VBM. We thus verify that, in this system, the last occupied band has an electron character in the central region of the Brillouin zone and a hole character elsewhere. We see from our calculated dispersion relations in Fig. 2(a) that the minimum hybridization gap occurs at some $\mathbf{k}_\parallel^*$ at $k_z=\pi/L_z$, and is 8 meV wide. In contrast, when $k_z=0$ the hybridization gap occurs at a slightly bigger $\mathbf{k}_\parallel^*$ and has a larger value of 25 meV.

In Fig. 2(b) we show the transition dipole matrix elements $|\langle\psi_{VBM}|\boldsymbol{\epsilon}\cdot\mathbf{p}|\psi_{CBM}\rangle|^2$ for the interband transitions between the last occupied state and the first unoccupied state at $\mathbf{k}_\parallel=0$ and at $\mathbf{k}_\parallel^*$. The position of the transitions is indicated by vertical arrows in Fig. 2(a). The transition dipole is calculated for different polarizations $\vec{\boldsymbol{\epsilon}}$ of the transitions: for in-plane polarizations $\vec{\boldsymbol{\epsilon}}=[110]$ and $\vec{\boldsymbol{\epsilon}}=[\bar{1}10]$ and for the out-of-plane component along the z direction, $\vec{\boldsymbol{\epsilon}}=[001]$. We note the following: (i) the transitions are stronger for in-plane momentum $\mathbf{k}_\parallel=\mathbf{k}_\parallel^*$ at the hybridization gap (i.e., $|\mathbf{k}_\parallel^*|\approx 2\times10^6\ \mathrm{cm}^{-1}$) than at $\mathbf{k}_\parallel=0$ ($\bar{\Gamma}$ point or $\bar{L}$ point). This is because the transitions at $\mathbf{k}_\parallel^*\neq0$ connect states that have amplitude both on the InAs segment and on the GaSb segment (see Fig. 3), while at $\mathbf{k}_\parallel=0$ the transitions connect a state localized on InAs to a state localized on GaSb, (thus being indirect in real space). (ii) While the transitions at $k_z=0$ are polarized mainly in plane, those at $k_z=\pi/L$ are polarized mainly along the z direction. (iii) The transitions at $\mathbf{k}_\parallel=\mathbf{k}_\parallel^*$ ($k_z=0$) show strong in-plane anisotropy (i.e., the intensity for $\vec{\boldsymbol{\epsilon}}=[110]$ is much stronger than for $\vec{\boldsymbol{\epsilon}}=[\bar{1}10]$ or vice versa). The anisotropy is particularly strong when the momentum $\mathbf{k}_\parallel^*$ is directed along the two in-plane (110) and ($\bar{1}10$) directions: the intensity of the transition polarized along the [110] ([$\bar{1}$10]) direction is an order of magnitude larger than that polarized along the [$\bar{1}$10] ([110]) direction when the momentum $\mathbf{k}_\parallel^*$ is along the [110] ([$\bar{1}$10]) direction. (iv) The polarization anisotropy is smaller for transitions at $\mathbf{k}_\parallel=0$ and at $\mathbf{k}_\parallel^*$ along the [100] and [010] in-plane directions.

B. Comparison of pseudopotential and k·p results

We have indicated in Fig. 2(a) the $\mathbf{k}\cdot\mathbf{p}$ results by crosses. Table I summarizes the important band gaps. As expected from Eq. (3b), for $\mathbf{k}_\parallel\neq0$ the agreement between the pseudopotential calculation and the pseudopotential-fit $\mathbf{k}\cdot\mathbf{p}$ calculation is very good: (i) The magnitude of the gaps at the Brillouin zone center ($\bar{\Gamma}$ and $\bar{L}$) and of the anticrossing gaps at $\mathbf{k}_\parallel^*$ are comparable. (ii) Both theories predict a much smaller

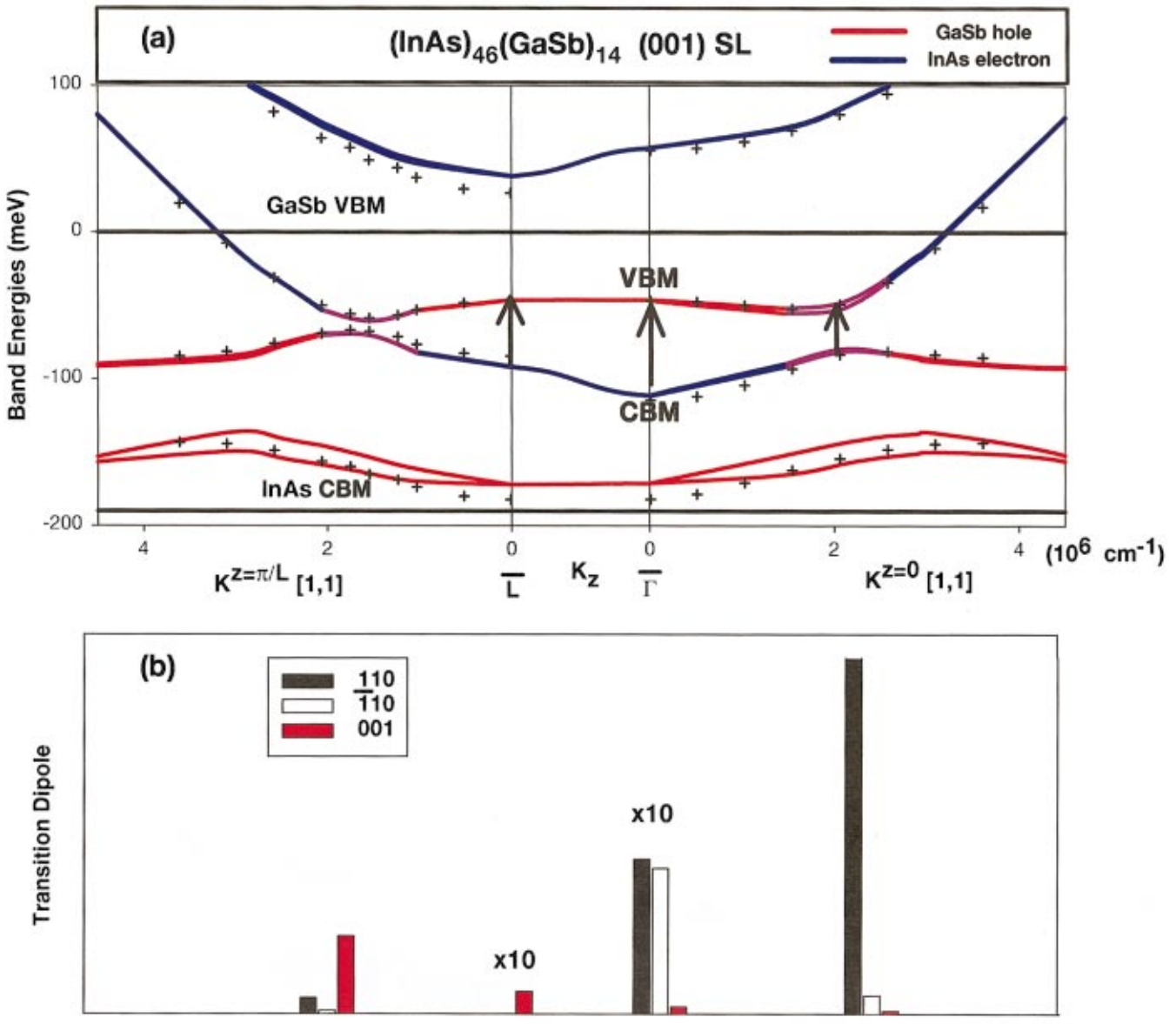

FIG. 2. (Color) The calculated dispersion relations for an $(InAs)_{46}(GaSb)_{14}$ (001) superlattice. Full lines are the pseudopotential results while crosses represent the 8×8 $\mathbf{k}\cdot\mathbf{p}$ results. Electron states localized on the InAs layer are depicted in blue, while the hole states localized on the GaSb layer are depicted in red. Horizontal lines denote the GaSb VBM and InAs CBM in the bulk.

anticrossing gap for the dispersion in $k_z=\pi/L_z$ relative to $k_z=0$. When its band parameters are drawn from the pseudopotential calculation the agreement between the two methods implies that the value of the matrix elements $V_{e,hh}^{EFA}(\mathbf{k}_\parallel\neq0)$ obtained in $\mathbf{k}\cdot\mathbf{p}$ [Eq. (3b)] are close to those for the atomistic pseudopotential calculation. We notice however, that the $\mathbf{k}\cdot\mathbf{p}$ method overestimates the dispersion of the ''CBM'' band along the k_z direction: the largest deviations between the two calculations occur at $\mathbf{k}_\parallel=0$.

C. The effect of the band offset

To estimate the effect of the GaSb-VBM vs InAs-CBM band offset (black horizontal lines in Fig. 2) on the hybridization gap, we show in Table I in parentheses the band-gap values obtained for the $(InAs)_{46}(GaSb)_{14}$ superlattice with the $\mathbf{k}\cdot\mathbf{p}$ method when the strained offset is changed from 190 meV (our present value[8]) to 150 meV. We see that while $E_H(\mathbf{k}_\parallel^*,k_z=0)$ changes relatively little ($\approx30\%$), $E_H(\mathbf{k}_\parallel^*,k_z=\pi/L_z)$ changes significantly (more than a factor of 5). Thus, the prediction of the anticrossing gaps magnitude at $k_z=\pi/L_z$ depends sensitively on the band-offset values. This is so because the (negative) gap at $\mathbf{k}_\parallel=0$ is smaller in magnitude for the smaller offset (150 meV), thus the anticrossing points $\mathbf{k}_\parallel^*$ occur closer to the Brillouin zone center, where the interaction $V_{e\text{-}hh}(\mathbf{k}_\parallel)$ is weaker, leading to a even smaller hybridization gap. Our smallest calculated hybridization gap occurs at $k_z=\pi/L_z$, and ranges from 1.5 meV (with a 150 meV offset) to 8 meV (with a 190 meV offset). It compares well with the ≈4 meV gap detected by Yang *et al.*[5] using capacitance-voltage measurements.

D. The effect of the superlattice period (n,m)

So far we discussed the period (46,14). In Fig. 4 we show how the hybridization gap changes when the individual layer

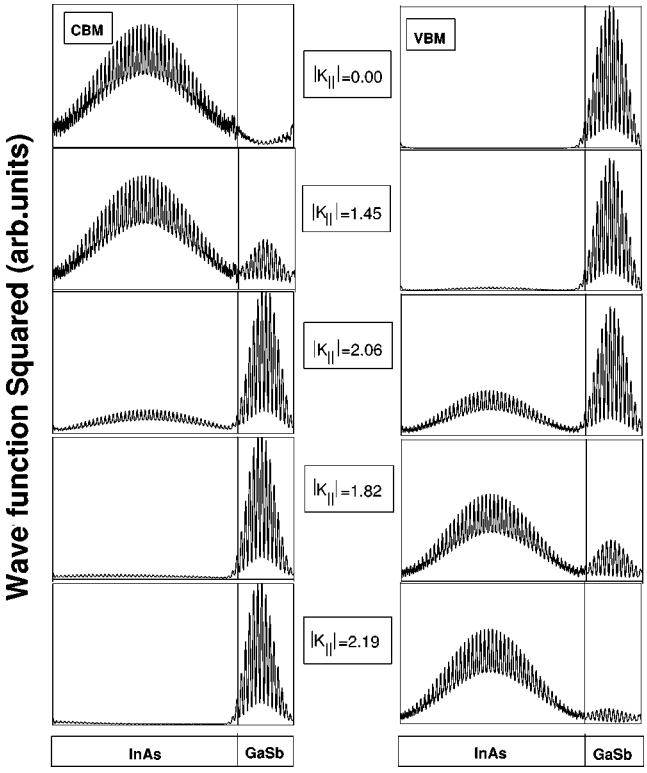

FIG. 3. Evolution of the wave function of the last occupied state (left column) and the first unoccupied state (right column) of the $(InAs)_{46}(GaSb)_{14}$ (001) superlattice along the in-plane $\mathbf{k}_\parallel=(k_x=k_y)$ direction at $k_z=0$. Wave functions are averaged over the in-plane coordinates.

thicknesses n and m are changed. We have considered a $(InAs)_{30}/(GaSb)_{30}$ superlattice with the same total $n+m$ period as the previously studied $(InAs)_{46}/(GaSb)_{14}$ superlattice. The pseudopotential calculated in-plane dispersion relations of the two superlattices along the $k_x=k_y$ direction at $k_z=0$ are compared in Fig. 4. Since the well widths determine the confinement energies, using the (30,30) period rather than (46,14) leads to a more confined electron (since the InAs electron well is now narrower) and to a less confined heavy hole (since the GaSb hole well is now wider). Thus, the (30,30) superlattice has a smaller (negative) gap at $\mathbf{k}_\parallel=0$ than the (46,14) superlattice. The negative gap at $\mathbf{k}_\parallel=0$ is now 17 meV, i.e., about one-fourth of the corresponding gap of the (46,14) superlattice. Since the electron and heavy-hole bands are already closer to each other at $\mathbf{k}_\parallel=0$ than in the (46,14) case, the anticrossing point $\mathbf{k}_\parallel^*$ occurs

TABLE I. Pseudopotential (P) and $\mathbf{k}\cdot\mathbf{p}$ calculated hybridization (H) gaps for a $(InAs)_{46}(GaSb)_{14}$ (001) superlattice. The band offset between the strained InAs CBM and GaSb VBM is 190 meV. In parentheses we give the band gaps obtained with a 150-meV offset.

Method	$E(\mathbf{k}_\parallel=0)$ (meV)		$E_H(\mathbf{k}_\parallel=\mathbf{k}^*)$ (meV)	
	$k_z=0$	$k_z=\frac{\pi}{L_z}$	$k_z=0$	$k_z=\frac{\pi}{L_z}$
P theory	65	45	25	8
$\mathbf{k}\cdot\mathbf{p}$	68(32)	38(8)	29(22)	8(1.5)

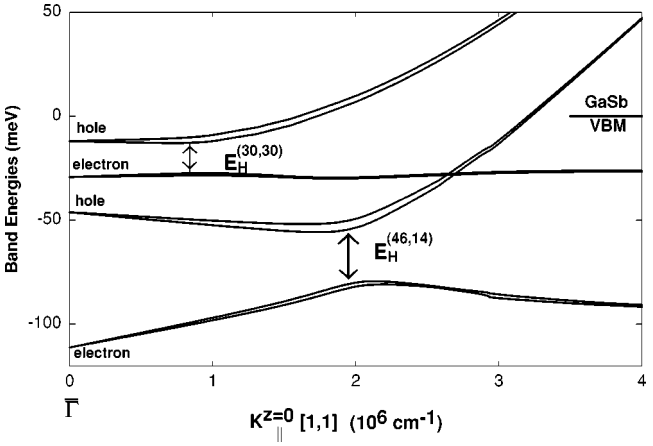

FIG. 4. Comparison between the pseudopotential calculated dispersion relations of a $(InAs)_{46}(GaSb)_{14}$ superlattice and of a $(InAs)_{30}(GaSb)_{30}$ along the $(k_x=k_y)$ direction at $k_z=0$.

closer to the Brillouin zone center. However, we see that the interaction $V_{e\text{-}hh}$ in this region given by the pseudopotential theory is relatively strong, and, as a consequence, the hybridization gap is 15 meV wide, not much smaller than the negative gap at $\mathbf{k}_\parallel=0$.

We have also examined the interband transition dipole matrix elements for the (30,30) superlattice and found that, while the transitions at $\mathbf{k}_\parallel=0$ have the same intensity as those in the (46,14) superlattice, both the intensity and the polarization anisotropy of the transitions at $\mathbf{k}_\parallel^*$ are smaller that those we have found in the (46,14) superlattice. Thus, we see that, the closer E_H is to $\mathbf{k}_\parallel=0$, the less intense and anisotropic are the interband transitions.

E. Comparison of pseudopotential and model calculations

Figure 5 compares the pseudopotential results with the model calculation of de-Leon *et al.*[6] for the $(InAs)_{46}(GaSb)_{14}$ system. The model of Ref. 6 describes the system as an InAs electron well interacting with a GaSb hole well, both wells being sandwiched between infinite barriers. Although two coupled quantum wells are a very simplified model of the system we are studying here, it is instructive to compare qualitatively our calculation with this model. The two systems are different in that the $(InAs)_{46}(GaSb)_{14}$ superlattice is a periodic system, showing a dispersion of the electron and hole bands along the k_z direction while there is no k_z dependence in the model of Ref. 6. The existence of the dispersion along k_z in our calculation reveals a coupling with other bands. In Ref. 6 the only allowed coupling is limited to the two electron and hole ground states of the uncoupled wells.

In Fig. 5 we compare the in-plane dispersions of the model in Ref. 6 with the superlattice dispersion for $k_z=0$. We see that the values of $\mathbf{k}_\parallel^*$ at the anticrossing points are similar in both calculations. We can think of our $k_z=0$ superlattice wave function as a periodic repetition of the corresponding quantum well wave function without any complication of additional phase factors. Now, however, in addition to the mixing due to the perturbation at the InAs/GaSb interface, which is present in the model of Ref. 6, we have an additional perturbation at the GaSb/InAs interface. As a re-

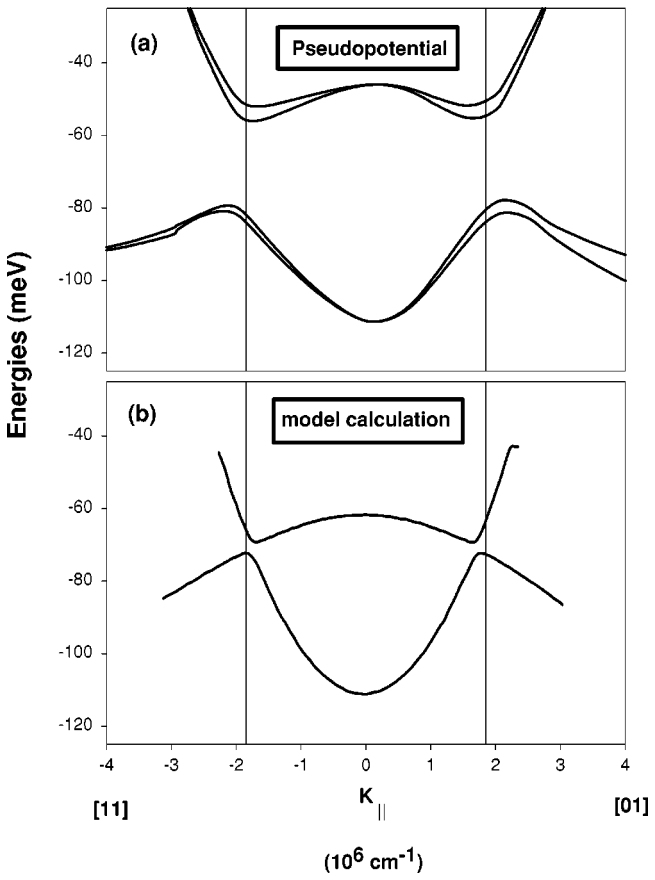

FIG. 5. Comparison between the in-plane dispersion of (a) the $(InAs)_{46}(GaSb)_{14}$ (001) superlattice calculated with the present pseudopotential method and (b) the coupled $(InAs)_{46}$ and $(GaSb)_{14}$ quantum wells of the model of de-Leon *et al.*, Ref. 6. The zero energy is at the GaSb VBM.

sult, the anticrossing gap at $\mathbf{k}_\parallel^*$ of the quantum well model of Ref. 6 should be doubled when it is compared with our superlattice result. Taking this into account, there is still a big difference between our directly calculated anticrossing gap of 22 meV (value corresponding to a 150-meV offset, which is the same offset used in Ref. 6) and the model's (doubled) value of about 7 meV. Thus we must conclude that the much smaller gap in the model calculation with respect to the pseudopotential calculation is due to the approximations introduced in the model.[6].

To examine the nature of these approximations, we note that the model introduces explicitly an interaction V_{IF} between InAs electron and GaSb hole states *only through* the interface (IF) boundary conditions. The model treats separately holes on one side (with a 4×4 $\mathbf{k}\cdot\mathbf{p}$ model) and electrons on the other, therefore missing the ''bulk'' contribution V_{BK} at $\mathbf{k}_\parallel\neq0$ of the elecron-hole interactions in the same material present in the full eight-band $\mathbf{k}\cdot\mathbf{p}$ method. The comparison between E_H in the model and in the pseudopotential (and $\mathbf{k}\cdot\mathbf{p}$) calculations shows that for $\mathbf{k}_\parallel\neq0$ this bulk interaction V_{BK} is important, while the interface related interaction, V_{IF} plays only a minor role. Indeed, inspection of the amplitude of our calculated wave functions *at the interface* (in Fig. 3) shows that it remains comparable to its value at $\mathbf{k}_\parallel=0$, even at the anticrossing point $\mathbf{k}_\parallel^*=0$. The observation that ''interface effects'' [related to the $V_{lh\text{-}hh}(\mathbf{k}_\parallel=0)$ and therefore to the $V_{e\text{-}hh}(\mathbf{k}_\parallel=0)$ coupling neglected in the $\mathbf{k}\cdot\mathbf{p}$ theory] on the E_H magnitude are small, leads to the conclusion that the $V_{e\text{-}hh}(\mathbf{k}_\parallel\neq0)$ coupling is not greatly affected by the $V_{e\text{-}hh}(\mathbf{k}_\parallel=0)$ coupling and, ultimately, by the interface symmetry effects. As a consequence, the nonequivalence of the interfaces in the $(InAs)_n/(GaAs)_n$ non-common-atom system influences the $\mathbf{k}\cdot\mathbf{p}$ results for the anticrossing gaps at $\mathbf{k}_\parallel\neq0$ less than those relative to other superlattice properties at $\mathbf{k}_\parallel=0$.

F. Are long-period $(InAs)_n/(GaSb)_n$ (001) superlattices indeed semiconducting?

Our foregoing discussion focusing on (46,14) and (30,30) superlattices showed that a single hybridization gap opens up at some $\mathbf{k}_\parallel^*\neq0$ value, thus rendering the nominally semimetallic superlattice a semiconductor, as suggested by Altarelli.[4] This is shown in Fig. 2(a) where the horizontal lines indicate the band edges of the bulk constituents, i.e., InAs CBM at $E=-190$ meV and GaSb VBM at $E=0$; we see but one anticrossing gap between these two horizontal lines. However, we find that for longer (n,m) periods, more than one hole state becomes higher in energy than the InAs CBM. This gives rise to ''multiple anticrossing minigaps,'' as already pointed out by Poulter *et al.*[7] Our calculations for a longer (50,34) superlattice shows indeed that at $\mathbf{k}_\parallel=0$ the electron state is at $E=-109$ meV, below four hole states (hh3 at -86 meV, lh1 at -71 meV, hh2 at -39 meV, and hh1 at -9 meV). Moving away from $\mathbf{k}_\parallel=0$ the electron state anticrosses with each of the higher hole states opening up minigaps at different energies and positions $\mathbf{k}_\parallel^*\neq0$. We find that two independent mechanisms are at work in determining a near metallization of the system. (1) Due to multiple anticrossings the band dispersions $E(\mathbf{k}_\parallel)$ undergo large distortions with sudden changes in their curvature, which are related to the change in character of the states (from hole to electron, then to hole again). These distortions can cause a hybridization gap to become strongly indirect and if the minimum of the higher band falls below the maximum of the lower band, then the semiconducting state will be distroyed. (2) If the Fermi level falls inside of one of these minigaps, and these gaps occur at the same energy in all $\mathbf{k}_\parallel$ directions at a given k_z, then the system, as a whole, will be a semiconductor. However, since the in-plane dispersions are different with respect to different $\mathbf{k}_\parallel$ directions, the small hybridization gaps generally occur at different energies, with no overlap between the various gaps. This, again, will lead to a gapless system. Thus, for long period superlattices the occurrence of out-of-phase multiple anticrossings is predicted to lead to a quasimetallic state, even in defect-free systems.

V. SUMMARY

In summary we have used a pseudopotential theory to study the in-plane $\mathbf{k}_\parallel$ dispersion relations of the last occupied state and the first unoccupied state in $(InAs)_n/(GaSb)_m$ superlattices. At some point $\mathbf{k}_\parallel^*\neq0$, which depends on the period (n,m), the two bands anticross forming a hybridization gap, and exhanging their localization in the InAs and GaSb wells. We find that (i) the magnitude and the position of the hybridization band gap $E_H^{n,m}(\mathbf{k}_\parallel,k_z)$ depend sensitively on

the period (n,m) and on the InAs CBM vs GaSb VBM offset, and (ii) the hybridization gap depends weakly (2–3 meV) on $\mathbf{k}_\parallel$, but strongly on k_z; it is smaller at $k_z=\pi/(n+m)a$ than at $k_z=0$. For example $E_H(\mathbf{k}_\parallel,k_z=0)=25$ meV while $E_H(\mathbf{k}_\parallel,k_z=\pi/L_z)=8$ meV for $(\mathrm{InAs})_{46}(\mathrm{GaSb})_{14}$. (iii) Although at $\mathbf{k}_\parallel=0$ the $\mathbf{k}\cdot\mathbf{p}$ model shows some important deviations[8] from the more accurate pseudopotential theory, for the in-plane dispersion $\mathbf{k}_\parallel\neq 0$, there is good agreement between the pseudopotential calculation and an eight-band $\mathbf{k}\cdot\mathbf{p}$ approach that uses input parameters extracted from the same pseudopotential bulk band structures. The largest deviation occurs at $\mathbf{k}_\parallel=0$, reflecting $V^{EFA}_{e,hh}(\mathbf{k}_\parallel=0)=0$. (iv) The $V^{EFA}_{e,hh}(\mathbf{k}_\parallel\neq 0)$ derived from the model calculation of de-Leon *et al.*[6] underestimates the hybridization gap by a factor of 3–4.

ACKNOWLEDGMENTS

We thank L. R. Ram-Mohan and Quantum Semiconductor Algorithms for use of the finite-element $\mathbf{k}\cdot\mathbf{p}$ software for the $\mathbf{k}\cdot\mathbf{p}$ calculations. Work at NREL was supported by the US DOE under Grant No. DE-AC36-98-Go10337, while work at NRL was supported by the Office of Naval Research.

[1] S.H. Wei and A. Zunger, Appl. Phys. Lett. **72**, 2011 (1998).
[2] L.L. Chang, J. Phys. Soc. Jpn. **49**, 997 (1980); L.L. Chang, N.J. Kawai, G.A. Sai-Halasz, R. Ludeke, and L. Esaki, Appl. Phys. Lett. **35**, 939 (1979).
[3] Y. Guldner, J.P. Vieren, P. Voisin, M. Voos, L.L. Chang, and L. Esaki, Phys. Rev. Lett. **45**, 1719 (1980).
[4] M. Altarelli, Phys. Rev. B **28**, 842 (1983).
[5] M.J. Yang, C.H. Yang, B.R. Bennett, and B.V. Shanabrook, Phys. Rev. Lett. **78**, 4613 (1997).
[6] S. de-Leon, B. Laikhtman, and L.D. Shvartsman, J. Phys.: Condens. Matter **10**, 8715 (1998); Phys. Rev. B **60**, 1861 (1999).
[7] A.J.L. Poulter, M. Lakrimi, R.J. Nicholas, N.J. Mason, and P.J. Walker, Phys. Rev. B **60**, 1884 (1999).
[8] L.W. Wang, S.H. Wei, T. Mattila, A. Zunger, I. Vurgaftman, and J.R. Meyer, Phys. Rev. B **60**, 5590 (1999).
[9] (a) G.H. Li, A. R. Goni, K. Syassen, O. Brandt, and K. Ploog, Phys. Rev. B **50**, 18 420 (1994); (b) M.H. Meynadier, R. E. Nahory, J. M. Worlock, M. C. Tamargo, J. L. de Miguel, and M. D. Sturge, Phys. Rev. Lett. **60**, 1338 (1988); (c) N.J. Pulsford, R. J. Nicholas, P. Dawson, K. J. Moore, G. Duggan, and C. T. B. Foxon, *ibid.* **63**, 2284 (1989).
[10] L.J. Sham and Y.T. Lu, J. Lumin. **44**, 207 (1989).
[11] L.W. Wang and A. Zunger, Phys. Rev. B **56**, 12 395 (1997).
[12] R.C. Miller, A.C. Gossard, G.D. Sanders, Y.C. Chang, and J.N. Schulman, Phys. Rev. B **32**, 8452 (1985).
[13] D.C. Reynolds, K.K. Bajaj, C. Leak, G. Peters, W. Theis, P.W. Yu, K. Alavi, C. Colvard, and I. Shidlovsky, Phys. Rev. B **37**, 3117 (1988).
[14] Y.C. Chang and J.N. Schulman, Appl. Phys. Lett. **43**, 536 (1983); Phys. Rev. B **31**, 2069 (1981).
[15] G. Edwards and J.C. Inkson, Solid State Commun. **89**, 595 (1994).
[16] D.M. Wood and A. Zunger, Phys. Rev. B **53**, 7949 (1996).
[17] O. Krebs and P. Voisin, Phys. Rev. Lett. **77**, 1829 (1996); O. Krebs, W. Seidel, J.P. Andre, D. Bertho, C. Jouanin, and P. Voisin, Semicond. Sci. Technol. **12**, 938 (1997).
[18] E.L. Ivchenko, A.Yu. Kaminski, and U. Rossler, Phys. Rev. B **54**, 5852 (1996).
[19] R. Magri and S. Ossicini, Phys. Rev. B **58**, R1742 (1998).
[20] E.L. Ivchenko, A.A. Toropov, and P. Voisin, Phys. Solid State **40**, 1748 (1998).
[21] M.G. Burt, J. Phys.: Condens. Matter **4**, 6651 (1992).
[22] B.A. Foreman, Phys. Rev. Lett. **82**, 1339 (1999).
[23] M.S. Hybertsen and S.G. Louie, Phys. Rev. B **35**, 5585 (1986).
[24] M. Cohen and V. Heine, in *Solid State Physics*, edited by H. Ehrenreich, F. Seitz, and D. Turnbull (Academic Press, New York, 1970), Vol. 24, p. 64.
[25] L.W. Wang and A. Zunger, J. Chem. Phys. **100**, 2394 (1994).
[26] L.R. Ram-Mohan and J.R. Meyer, J. Nonlinear Opt. Phys. Mater. **4**, 191 (1995).
[27] G.C. Dente and M.L. Tilton, J. Appl. Phys. **86**, 1420 (1999).